

## MODIFICATION OF DIODE CHARACTERISTICS BY ELECTRON BACK-SCATTER FROM HIGH-ATOMIC-NUMBER ANODES\*

D. Mosher, G. Cooperstein, D.V. Rose<sup>+</sup>, and S.B. Swanekamp<sup>+</sup>

*Plasma Physics Division, Naval Research Laboratory, Washington, DC, 20375, USA*

In high-power vacuum diodes with high-atomic-number anodes, back-scattered electrons alter the vacuum space charge and resulting electron and ion currents. Here, electron multiple back-scattering is studied through equilibrium solutions of the Poisson Equation for 1-dimensional, bipolar diodes in order to predict their early-time behavior. Before ion turn-on, back-scattered electrons from high-Z anodes suppress the diode current by about 10%. After ion turn-on in the same diodes, electron back-scatter leads to substantial enhancements of both the electron and ion currents above the Child-Langmuir values. Current enhancements with ion flow from low-Z anodes are small.

In high-power vacuum diodes with high-atomic-number (high-Z) anodes, a large fraction of the electrons are back-scattered, thereby altering the space charge in the vacuum gap and the resulting electron and ion currents from their conventional values. This process may contribute to observed differences in the early-time behavior of pinched-beam diodes (PBDs) with low-Z and high-Z anodes in NRL Gamble II experiments.<sup>1</sup> Here, electron multiple back-scattering is studied through equilibrium solutions of the Poisson Equation for 1-dimensional (1D), bipolar diodes in order to model behavior prior to pinching. The treatment builds on a model developed by Pereira.<sup>2</sup> An analytic approximation to the back-scattered distribution described by electron-current and -energy parameters provides a first integral of the Poisson Equation that is solved numerically to determine how the diode currents are modified for various assumed back-scatter coefficients. A Monte-Carlo code calculates the back-scattered electron distributions for various incident electron distributions and anode materials. The back-scatter parameters used in the Poisson analysis are then evaluated from the Monte-Carlo results to determine the back-scatter-modified diode currents.

The starting point is the nonrelativistic Poisson Equation in 1D in which cold electrons are emitted from the cathode at  $z = 0$ , accelerated across the diode with potential variation  $\phi(z)$ , and enter the anode at  $z = d$  and  $\phi = V$ . A fraction  $\alpha$  of the incident electron current is isotropically back-scattered with energy reduced from the incident value  $eV$  to  $\beta eV$ . Since  $\beta < 1$ , back-scattered electrons are returned to the anode by the diode electric field, and the back-scattering process is assumed to repeat ad infinitum with the same values of  $\alpha$  and  $\beta$ . With these assumptions, the Poisson Equation can be integrated analytically to yield

$$B \left( \frac{d\Phi}{d\xi} \right)^2 = \Phi^{1/2} - \left( \frac{M}{m} \right)^{1/2} \left( \frac{J_i}{J_e} \right) (1 - \sqrt{1 - \Phi}) + \frac{4}{3} \sum_{n=1}^{\Phi > 1 - \beta^n} \left( \frac{\alpha}{\beta} \right)^n (\Phi - 1 + \beta^n)^{3/2} \quad (1)$$

where  $B = (2eV/m)^{1/2} V / 4\epsilon_0 J_e d^2$ ,  $m$  and  $M$  are the electron and ion mass,  $\xi = z/d$ ,  $\Phi = \phi/V$ , and  $J_e$  and  $J_i$  are the magnitudes of the electron and ion current densities traversing the diode. The boundary conditions  $\Phi(0) = \Phi'(0) = 0$ , and  $\Phi(1) = 1$  have been employed in Eq. (1).

\* Work supported by the Office of Naval Research, USA.

+ JAYCOR, Vienna, VA

The first two terms on the right-hand-side are the familiar forms that follow from conservation of energy and current in 1D for cold, laminar electron and ion flows with zero electron energy at the cathode and zero ion energy at the anode.<sup>3</sup> The last term follows for multiple, isotropic back-scattering of monoenergetic electrons.<sup>2</sup> This 1D formalism approximates early-time charged-particle flow in Gamble II PBD experiments before the electron beam pinches radially.<sup>1</sup>

Before ion turn-on,  $J_i = 0$  in Eq. (1), and  $J_e$  is determined from the value of  $B$  that permits the two boundary conditions on  $\Phi$  to be satisfied when the equation is integrated numerically for various  $\alpha$  and  $\beta$  values. Figure 1 plots the variation of  $J_e/J_{cl}$  for these calculations, where  $J_{cl}$  is the usual Child-Langmuir current density ( $B = 9/4$ ). The results indicate that back-scattering suppresses the current by 5 - 20% for values of  $\alpha$  and  $\beta$  associated with high-atomic-number anodes (0.3 - 0.7 for tantalum depending on incident energy and angle<sup>4</sup>). For low-atomic-number anodes such as aluminum or carbon,  $\alpha$  and  $\beta$  are of order 0.1 and suppression is negligible. The equivalent relativistic calculations show little difference from Fig. 1 for diode voltages in the 1-MeV range of interest. The nonrelativistic treatment is therefore employed since the results are then not voltage dependent. The weak suppression predicted for moderate  $\alpha$  and  $\beta$  values arises because  $\beta$  close to 1 is required for a substantial back-scattered-electron contribution to space charge near the cathode.

When ion emission is included in the analysis, the ion-to-electron current ratio is determined by space-charge-limited flow at the anode:  $\Phi'(1) = 0$ . Substituting this condition into Eq. (1) leads to

$$\left(\frac{M}{m}\right)^{1/2} \frac{J_i}{J_e} = \frac{1 + \alpha\beta^{1/2}/3}{1 - \alpha\beta^{1/2}} ; \quad \frac{J_i}{J_{cl}} = \frac{J_i}{J_e} \frac{J_e}{J_{cl}} \quad (2)$$

where the converging infinite series has been evaluated analytically. The current ratio from Eq. (2) is substituted into Eq. (1) to determine the value of  $B$  as above, and the results are shown in Fig. 2. For small values of  $\alpha$ , electron and ion currents are enhanced by a factor of 1.86 as expected for 1D, bipolar flow.<sup>3</sup> For  $\alpha$  and  $\beta$  values of high-atomic-number anodes, large enhancements in both electron and ion current are predicted. In this regime, back-scattered-electron space charge near the anode enhances ion emission which, in turn, enhances cathode electron emission. This boot-strap process causes enhancement to increase dramatically with small increases in  $\alpha$  near  $\beta = 0.5$ . Further small increases in  $\alpha$  cause the enhancement to approach infinity, beyond which no equilibrium solutions to Eq. (1) exist that satisfy the boundary conditions. Mathematically, the no-solution regime corresponds to potential distributions with an extremum in the vacuum gap so that the dependence of charge

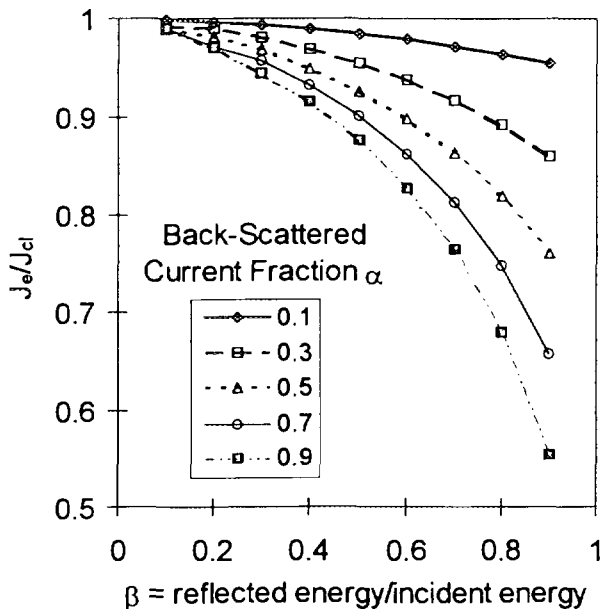


FIG. 1. Suppression of electron current with back-scattering parameters in the absence of ions.

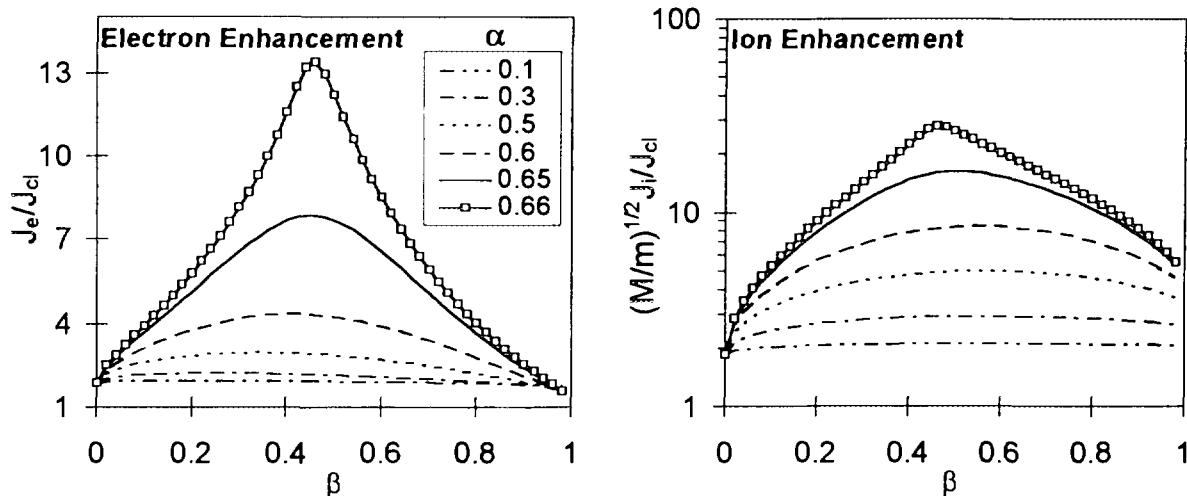


FIG. 2. Enhancement of bipolar electron and ion current with back-scattering parameters.

density on  $\Phi$  is no longer valid. Physically, this regime may correspond to inherently time-dependent flows<sup>5</sup> that describe a low-impedance phase observed in PBDs.<sup>6</sup> The no-solution regime, shown in Fig. 3, has been calculated by determining the portion of  $(\alpha, \beta)$  space for which  $\Phi'(\xi) = 0$  somewhere between the electrodes.

Having calculated how the charged-particle flow depends on monoenergetic, isotropic back-scatter parameters, it remains to compare this assumed electron distribution with computed, more realistic forms. The Integrated TIGER Series of Monte Carlo electron/photon transport codes<sup>7</sup> was used to determine the back-scattered-electron distributions for various incident-electron energies, angles and anode materials. A sample result of TIGER calculations is shown in Fig. 4 for electrons with  $E_0 = 1$  MeV incident on Ta at  $\theta_0 = 60^\circ$ . Here,  $R$  is the number fraction of incident electrons that are back-scattered,  $E$  is their energy,  $\theta$  is the angle from the normal at which they emerge, and  $d\Omega$  is a solid-angle increment. With  $f(E, \theta) = d^2R/dEd\Omega$ ,  $R = \int f dEd\Omega$ , and  $RE_0 \langle \beta \rangle = \int f E dEd\Omega$ . These calculations show that  $R$  and  $\langle \beta \rangle$  depend weakly on  $E_0$  over the range 0.2 - 2 MeV so that the assumption of constant back-scatter coefficients during multiple

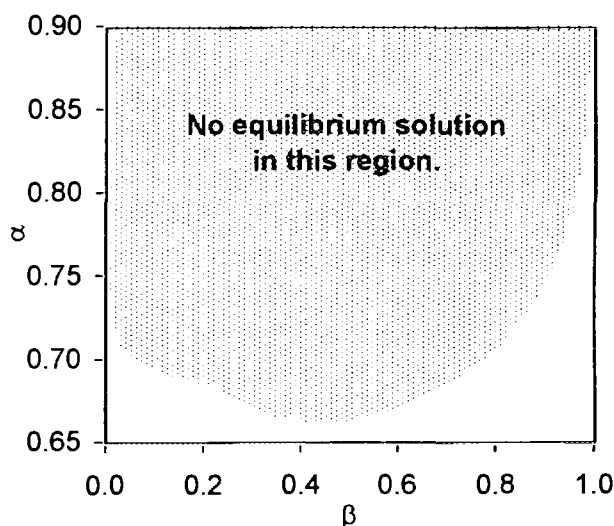


FIG. 3. Back-scatter parameters without equilibrium solutions.

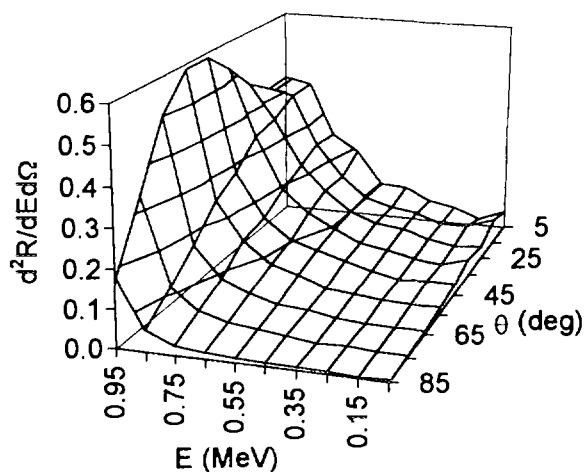


FIG. 4. Back-scattered electron distribution for 1-MeV electrons incident on Ta at 60 degrees.

scattering is reasonable. For 1 MeV electrons incident on Ta,  $R$  and  $\langle\beta\rangle$  vary from 0.46 to 0.64 and 0.32 to 0.5 as  $\theta_0$  varies from 0 to  $60^\circ$ .

In order to determine  $\langle\alpha\rangle$  and compare the TIGER results to the model of Eq. (1), the data exemplified by Fig. 4 is collapsed to an axial-velocity distribution. The plotted points represent the number-fractions  $\Delta R_{ij}$  of electrons scattered into energy increments  $\Delta E = 0.1$  MeV about  $E_i$  and into solid-angle increments  $\Delta\Omega_j = 2\pi\sin\theta_j\Delta\theta$  with  $\Delta\theta = 10^\circ$ . Each  $\Delta R_{ij}$  has a relativistic axial velocity  $v_z$  determined from  $E_i$  and  $\cos\theta_j$ . These are sorted in  $v_z$  and summed in  $\Delta v_z = 0.1v_0$  bins, where  $v_0$  is the incident electron speed. The results are shown in Fig. 5 for 1-MeV electrons incident on Ta. For comparison with the model used in Eq. (1), the axial velocity has been normalized by  $w = v_z/v_0$ , and the distribution  $g(w) = (1/R)dR/dw$  is used so that the integral over  $w$  is unity. Poor statistics in  $\Delta w$  bins results from the coarse TIGER  $\Delta E$  and  $\Delta\theta$  gridding. The isotropic/monoenergetic distributions use the TIGER  $\langle\beta\rangle$  values and display constant  $dR/dw$  up to  $w = \langle\beta\rangle^{1/2}$  since  $d\Omega \sim \sin\theta d\theta \sim d(\langle\beta\rangle\cos\theta) = dw$ .

The TIGER  $w$ -distributions determine  $\langle\alpha\rangle$ , the ratio of back-scattered to incident current, using  $\langle\alpha\rangle = R\langle w\rangle/\cos\theta_0$ , where  $\langle w\rangle = \int g(w)w dw \approx 0.6$ . For 1-MeV electrons incident on Ta,  $\langle\alpha\rangle$  varies from about 0.3 to 0.75 as  $\theta_0$  varies from 0 to  $60^\circ$ . Since ion turn-on usually occurs when the anode is heated by electrons magnetically deflected to steep incident angles, the large corresponding values of  $\langle\alpha\rangle$  and  $\langle\beta\rangle$  and Fig. 2 indicate large current enhancements. This results will be mediated by differences between the realistic TIGER back-scattered distributions and the nonrelativistic, isotropic model used in Eq. (1). Figure 5 shows that the model overestimates the contribution by electrons with low  $w$  and underestimates those with large  $w$ . Excess low- $w$  electrons increase the electron space charge near the anode, thereby enhancing ion emission. Insufficient high- $w$  electrons reduce the electron space charge near the cathode, thereby increasing electron emission. Both effects indicate that more realistic, back-scattered-electron distributions will reduce the enhancements determined from the solution of Eq. (1) bringing them closer to Pereira's values.<sup>2</sup> For the future, it is desired to combine a particle-in-cell (PIC) code with a Monte-Carlo treatment to examine time-dependent diode behavior in the no-solution regime.

The authors acknowledge helpful discussions with M. Desjarlais.

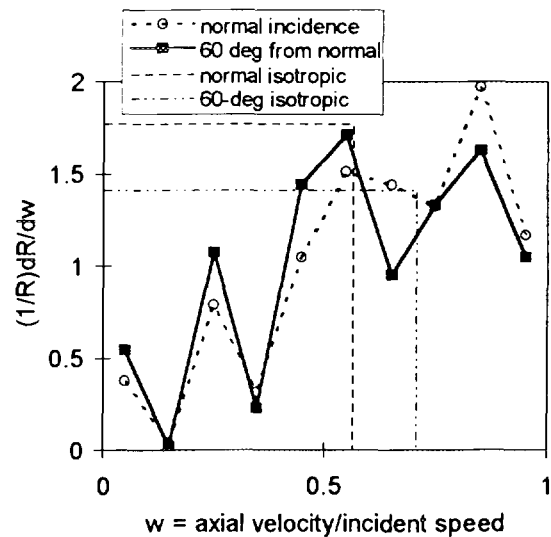


FIG. 5. Normalized axial-velocity distributions for 1-MeV electrons incident on Ta.

- [1] G. Cooperstein, *et al.*, these Proc. See D.J. Johnson and S.A. Goldstein, *J. Appl. Phys.* **48**, 2280(1977).
- [2] N.R. Pereira, *J. Appl. Phys.* **54**, 6307(1983).
- [3] L. Langmuir, *Phys. Rev.* **33**, 954(1929).
- [4] A. Pregoner and J.E. Morel, *J. Appl. Phys.* **57**, 4849(1985).
- [5] H. Derfler and R. Holmstrom, *J. Appl. Phys.* **37**, 4189(1966).
- [6] Cooperstein, *et al.*, *Bull. Am. Phys. Soc.* **23**, 800(1978).
- [7] J.A. Halbleib, R.P. Kensek, G.D. Valdez, S.M. Seltzer, and M.J. Berger, *IEEE Trans. Nucl. Sci.* **39**, 1025(1992).